



Efficiency, mechanism and microbial community of Cd(II) removal by mixed bacteria enriched from heavy metals mine soil

Tao-tao ZENG¹, Xiao-ling ZHANG¹, Hai-du NONG¹, Qing HU¹, Liang-qin WANG¹, Ai-jie WANG²

1. Hunan Provincial Key Laboratory of Pollution Control and Resources Reuse Technology,
University of South China, Hengyang 421001, China;

2. Key Laboratory of Environmental Biotechnology, Chinese Academy of Sciences, Beijing 100085, China

Received 21 August 2021; accepted 20 January 2022

Abstract: Mixed bacteria were enriched from heavy metals mine soil for cadmium (Cd(II))-containing wastewater treatment. Batch adsorption experiment results showed that the optimal pH, temperature, initial Cd(II) concentration, and biomass dosage were 6.0, 30 °C, 20 mg/L, and 1 g/L, respectively. Living biomass exhibited better Cd(II) removal efficiency (91.97%) than autoclaved biomass (79.54%) under optimal conditions. The isotherms and kinetics of living biomass conformed to the Langmuir isotherm model and pseudo-first-order kinetic model, respectively. FTIR results implied that amine groups, hydroxyl groups and phosphoric acid play an important role in the Cd(II) adsorption process, while XRD results showed that crystalline Cd(OH)₂ and CdO were obtained. After Cd(II)-containing wastewater treatment exposure, the dominant bacteria genera included *Comamonas* (39.94%), *unclassified_f_Enterobacteriaceae* (34.96%), *Ochrobactrum* (14.07%), *Alcaligenes* (4.84%), *Bordetella* (2.07%), *Serratia* (1.04%), and *Bacillus* (1.01%). Function prediction showed that the abundance of metabolic genes changed significantly. This study proposes the potential application of mixed bacteria for Cd(II)-containing wastewater treatment.

Key words: Cd(II); wastewater treatment; bacterial community; function prediction

1 Introduction

Heavy metal (HM) contamination in water, sediments and soils, resulting from mining, smelting and sewage irrigation, is becoming an increasingly serious problem worldwide, causing adverse effects on human health and environmental sustainability [1,2]. Cadmium (Cd(II)) is one of the most concerning HMs due to its highly toxic effects considering its extensive use and persistence, being difficult to remove by degradation or migration [3]. Cd is widely utilized in various industries, such as electroplating [4], mining [5] and plastics manufacturing [1], with concentrations ranging from 10 to 100 mg/L. According to the Chinese

Integrated Wastewater Discharge Standard (GB 8978—1996), the maximum permissible effluent Cd(II) concentration should be less than 0.1 mg/L [6], therefore, wastewater contaminated with Cd(II) generally requires treatment.

The conventional methods of Cd(II) removal include chemical precipitation [7] and ion-exchange [8], both of which are highly efficient, but with the drawbacks of high reagent and energy requirements and the generation of secondary pollution. Bioremediation technologies have been found to be promising for Cd(II) removal with the advantages of low cost and low environmental impact [9]. Previous reports [3,4,9,10] have found that microorganisms such as bacteria, fungi, and algae have high-efficiency adsorption capabilities

Corresponding author: Tao-tao ZENG, Tel: +86-734-8282312, E-mail: biowater@126.com;

Ai-jie WANG, Tel/Fax: +86-10-62925515, E-mail: ajwang@rcees.ac.cn

DOI: 10.1016/S1003-6326(22)66028-X

1003-6326/© 2022 The Nonferrous Metals Society of China. Published by Elsevier Ltd & Science Press

for Cd(II). The bacterial species commonly isolated when evaluating the optimum conditions for Cd(II) biosorption from different metal contaminated sites were *Pseudomonas* sp. 375 [3], *Plesiomonas shigelloides* [11], *Bordetella petrii* [12], *Bacillus cereus* RC-1 [13], *Vibrio alginolyticus* PBR1 [14], *Bacillus* sp. C9-3 [15], and *Comamonas* sp. XL8 [16]. The Cd(II) biosorption capacities (q_{\max}) of living and nonliving *Pseudomonas* sp. 375 were 92.59 and 63.29 mg/g, respectively, with the mechanism involving Cd(II) being tightly bound onto the cell wall by various groups such as —OH, —SO₃²⁻ and —NH₂ [3]. It has also been reported that Cd(II) uptakes by live and dead *Chlorella vulgaris* cells were 16.34 and 16.65 mg/g, respectively, with the adsorption process fitting a pseudo first-order kinetic model [9]. The biosorption of Cd(II) by dried *Aphanothece* sp. was found to be spontaneous and exothermic, with at least 9 functional groups interacting with Cd(II) and cation exchange being the main biosorption mechanism [17]. However, most previous studies on Cd(II) biosorption focused on the removal effect of a single bacterium in isolation, while few studies have investigated Cd(II) adsorption by multiple co-occurring bacteria, despite these systems exhibiting higher removal potential and a greater capacity to adapt to complex wastewater environments.

Therefore, the present study aims to explore: (1) the enrichment of the multiple bacteria from HM mine soil and the effects of different operational parameters on the Cd(II) removal efficiency of living and autoclaved bacterial biomass (pH, temperature, initial Cd(II) concentration and biomass dosage); (2) the Cd(II) biosorption mechanism using isotherm and kinetic model fitting, to characterize the microstructures and functional groups involved in biosorption; (3) the bacterial community composition, phylogenetic analysis and function prediction for the enriched bacteria.

2 Experimental

2.1 Bacterial enrichment and biomass collection

To ensure effective enrichment of Cd(II) resistant bacteria, the soil was collected from a HMs mine site in Southern China. The sampled soil contained an excess of multiple HMs including Cd,

Pb, Zn, As, and Cu. After being passed through a sieve with 2.54 mm pore size, 10 g of soil was dissolved in 90 mL distilled water and stirred to form a homogenous mixture, the supernatant was then inoculated into liquid growth medium (5 g/L beef extract, 10 g/L tryptone and 10 g/L sodium chloride, at pH 7.2), and then cultured for 24 h at 30 °C. The culture was spread on Luria-Bertani (LB) medium agar plates and maintained at 30 °C until visible bacterial colonies could be observed.

All the visible colonies were collected and transferred into separate flasks containing LB liquid medium and cultured at 30 °C, with continual agitation at 150 r/min until growth entered the stationary phase (48 h). The bacterial culture solution was then harvested by centrifugation at 8000 r/min and 4 °C for 10 min, obtaining a viable cell pellet, which was washed three times with sterile water. To harvest inactive cells, the bacterial cultures were autoclaved at 121 °C for 20 min, then centrifuged and washed as described above. Both living and autoclaved cell pellets were freeze-dried at -60 °C using freeze dryer (LGJ-50FG, Beijing Yaxing Science Technology Development Co., Ltd., China) for 24 h to obtain living and autoclaved biomass, then stored at 4 °C prior to use in batch experiments.

2.2 Batch biosorption experiments

Batch biosorption experiments were performed using both living and autoclaved biomass in 50 mL flasks containing 20 mL Cd(II) solution. The effects of abiotic operational parameters on Cd(II) biosorption were assessed, including pH (3.0–8.0), temperature (25, 30, 35, and 45 °C), initial Cd(II) concentration (10–100 mg/L) and biomass dosage (0.5–3 g/L). All experiments were performed for 168 h to establish the optimum adsorption time and abiotic parameter conditions, with the optimum conditions then utilized for experiments comparing living and autoclaved biomass to explore the adsorption efficiency and mechanism. All experiments were performed in triplicate and conducted alongside control experiments without the addition of the living or autoclaved biomass.

2.3 Kinetics and isotherm of biosorption

In order to describe biosorption equilibrium and calculate the biosorption capacity, Langmuir and Freundlich isotherms were applied to analyzing

the experimental data [3]. Isotherm experiments were carried out using different initial Cd(II) concentrations (10–100 mg/L) at an initial pH of 6, biomass dosage of 1 g/L and 30 °C. The analysis of the adsorption kinetics is essential to establish the adsorption mechanism and rate-limiting steps [18]. Therefore, pseudo-first-order and pseudo-second-order kinetic models were used to analyze the adsorption process dynamics of biomass containing 20 mg/L Cd(II), with removal assessed at an initial pH of 6, 1 g/L biomass dosage and reaction temperature of 30 °C.

2.4 Multiple HM co-adsorption experiments

Cd(II), Pb(II), Zn(II), Cu(II), and Mn(II) were added to wastewater collected from the Pinewood Sewage Treatment Plant (Hengyang City, Hunan Province, China). Cd(II), Pb(II), Zn(II), Cu(II), and Mn(II) concentrations were adjusted according to the average wastewater concentrations reported previously in Refs. [1–11] in the Supplementary Materials (Table S1) with final concentrations of 9.5 mg/L Cd(II), 8.2 mg/L Pb(II), 3.4 mg/L Zn(II), 2.9 mg/L Cu(II), and 8.1 mg/L Mn(II). The supplemented wastewater was combined with 1.5 g/L living or autoclaved biomass and the adsorption experiments were maintained for 120 h thereafter. The concentrations of HMs (Cd(II), Pb(II), Zn(II), Cu(II), and Mn(II)) remaining in the supernatant after centrifugation at 8000 r/min for 10 min and filtration through a nylon filter (0.22 µm, Jin Nong, Ni Nong 66, China) were determined by a flame atomic adsorption spectrophotometry (FAAS, AA-6300, Shimadzu, Japan).

2.5 Characterization of biosorption mechanism and functional bacterial community

2.5.1 Cd(II) biosorption sites

There are three mechanisms of HM removal by bacterial cells: loose binding, tight binding, and intracellular accumulation [3]. The sites of Cd(II) biosorption by bacteria were established after exposure to 20 mg/L Cd(II) for 120 h, then quantitatively analyzed according to modified versions of previously reported methods [13], as described in detail in Section 1 and Fig. S1 in the Supplementary Materials.

2.5.2 Micromorphology and functional group analysis

Micromorphological and elemental analysis of the living and autoclaved biomasses was performed before and after Cd(II) exposure by scanning electron microscopy coupled with energy dispersive X-ray analysis (SEM-EDS, Zeiss Ultra Plus-360, Germany). The biomass surface functional groups were characterized by Fourier transform-infrared red spectroscopy (FTIR, Thermo Scientific Nicolet 6700, USA) with scanning performed within a wavenumber range from 4000 to 400 cm⁻¹ [19]. Crystal structure identification was carried out using X-ray diffractometry (XRD, Rigaku Ultima IV, Japan).

2.5.3 Bacterial community characterization and gene functional prediction

The initial and the post-reaction biomasses following exposure to 20 mg/L Cd(II), were homogenized separately and the genomic DNA was then extracted using the E.Z.N.A. Soil DNA Kit (OMEGA, BioTek, Winooski, VT, USA) according to the manufacturer's instructions. The V4 hypervariable region of the 16S rRNA gene was amplified using the 515FmodF and 806RmodR primers [20]. High-throughput sequencing was performed using an Illumina MiSeq platform by Shanghai Majorbio Bio-pharm Technology Co., Ltd., China.

After quality control to remove short fragments and low-quality sequences that did not meet the requirements [21], the obtained sequences were classified into operational taxonomic units (OTUs) at a 97% similarity threshold, using Usearch software v. 7.0 (<http://drive5.com/uparse/>). Taxonomic assignment was performed using RDP Classifier software v. 2.6, establishing the bacterial community composition and abundance at the genus level. The phylogenetic tree was constructed using MEGA7.0 (<https://www.megasoftware.net/history.php>) according to the neighbor-joining method [22]. The prediction of bacterial function was performed using the PICRUSt program based on the Clusters of Orthologous Groups of proteins (COG, <http://www.ncbi.nlm.nih.gov/COG/>) and Kyoto Encyclopedia of Genes and Genomes (KEGG, <http://www.genome.jp/kegg/>) databases [23]. The sequences were submitted to the Sequence Read Archive (SRA) database of the National Center of Biotechnology Information (NCBI) under the accession number SRR15100553-SRR 15100554.

2.6 Statistical analysis

The concentration of Cd(II) in the solution was analyzed by FAAS after centrifugation (10000 r/min, 5 min) and filtration through a 0.22 μm membrane. The Cd(II) removal efficiency was calculated according to Eq. (1), while the biosorption capacity was determined based on the amount of Cd(II) adsorbed per unit of biosorbent as per Eq. (2) [24]:

$$R = (C_0 - C_i) / C_0 \times 100\% \quad (1)$$

$$q = (C_0 - C_e) V / m \quad (2)$$

where R is the removal efficiency, q is the adsorption capacity (mg/g); C_i , C_0 , and C_e are the Cd(II) concentrations (mg/L) at time i , initial and equilibrium, respectively; V is the solution volume (L); m is the mass of biomass used in the experiment (g).

Data analysis and graph plots were performed using Excel (Microsoft 2019) and OriginPro 2017, respectively. All experiments were performed in triplicate and results were expressed as mean value \pm SD, while the statistical significance of results was analyzed using one-way analysis of variance (ANOVA) combined with Duncan's test ($p < 0.05$) analysis.

3 Results and discussion

3.1 Bacteria enrichment and Cd(II) resistance

The growth curve for the enriched bacteria is shown in Fig. S2(a). The bacteria quickly entered the logarithmic growth phase with almost no lag period, with the stable period occurring from 24 h. The Cd(II) tolerance test results are shown in Fig. S2(b). Upon exposure to 1 mmol/L Cd(II), the enriched bacteria entered a 6 h lag period, followed by a 18 h logarithmic phase, reaching a stable growth period at 24 h. These results indicate that the enriched bacteria were tolerant to exposure to 1 mmol/L Cd(II). Following exposure to 2 mmol/L Cd(II), the enriched bacteria failed to show any signs of growth. In a previous report, SHI et al [16] isolated *Comamonas* sp. XL12 and XL15 from soil collected at Daye Iron Ore Mine (Huangshi City, Hubei Province, China), with an inhibition effect observed with exposure to 0.25 mmol/L Cd(II) solution. In comparison, the enriched bacteria in the present study exhibited higher Cd(II) tolerance, verifying that the bacterial biomass was a promising

biosorbent for Cd(II) removal in the following batch tests.

3.2 Biosorption experiment results

3.2.1 Effect of initial pH

The effect of pH on Cd(II) removal by living biomass is shown in Fig. 1(a). After 120 h of adsorption, 91.97% of Cd(II) was removed by living biomass at an initial pH of 6. It was observed that the biosorption rate reduced when the pH was higher or lower than 6. It has been reported that solution pH significantly affects living bacteria biosorption by altering the availability of adsorption sites [24]. Under low pH conditions ($\text{pH} < 6$), Cd(II) and H^+ compete for active binding sites on the biosorbent surface, especially at pH 3, due to the large number of H^+ ions available [17,25]. With increasing pH, the concentration of H^+ in solution decreased, weakening the competition and increasing Cd(II) removal. However, when the solution $\text{pH} > 8$, the speciation of Cd changed significantly, existing in the form of CdOH^+ , resulting in a decrease in removal rate (Fig. S3) [26]. In addition, variation between neutral and alkaline environments has been shown to affect the activity of living biomass, reducing the removal rate under high pH conditions [27]. Therefore, the results of the present study are in agreement with previously reported studies on Cd(II) biosorption by bacteria [3], with optimal adsorption occurring at pH 6, which was set as the initial pH for all subsequent adsorption tests.

3.2.2 Effect of adsorption temperature

The effect of varying temperatures (25–40 $^{\circ}\text{C}$) on Cd(II) adsorption by living biomass is presented in Fig. 1(b). Data show that from the 1st day to the 7th day, Cd(II) removal efficiencies increased from 23.23% to 74.68%, 35.54% to 91.97%, and 50.37% to 79.93% at 25, 30, and 35 $^{\circ}\text{C}$, respectively. While at 40 $^{\circ}\text{C}$, the Cd(II) removal efficiency increased to 55.99% on the 1st day, 70.10% on the 4th day and then decreased to 66.02% on the 7th day. It was found that under higher temperature conditions, the Cd(II) removal efficiency was enhanced in the first 2 d, while after 4 d, the fastest increase in Cd(II) removal efficiency occurred at 30 $^{\circ}\text{C}$, reaching 91.97% removal by the 7th day. ARIVALAGAN et al [28] isolated the Cd(II) tolerant bacteria *Bacillus cereus* from soil surrounding an industrial electroplating site, exhibiting a maximum Cd(II) biosorption capacity of 82% at pH 6 and 35 $^{\circ}\text{C}$.

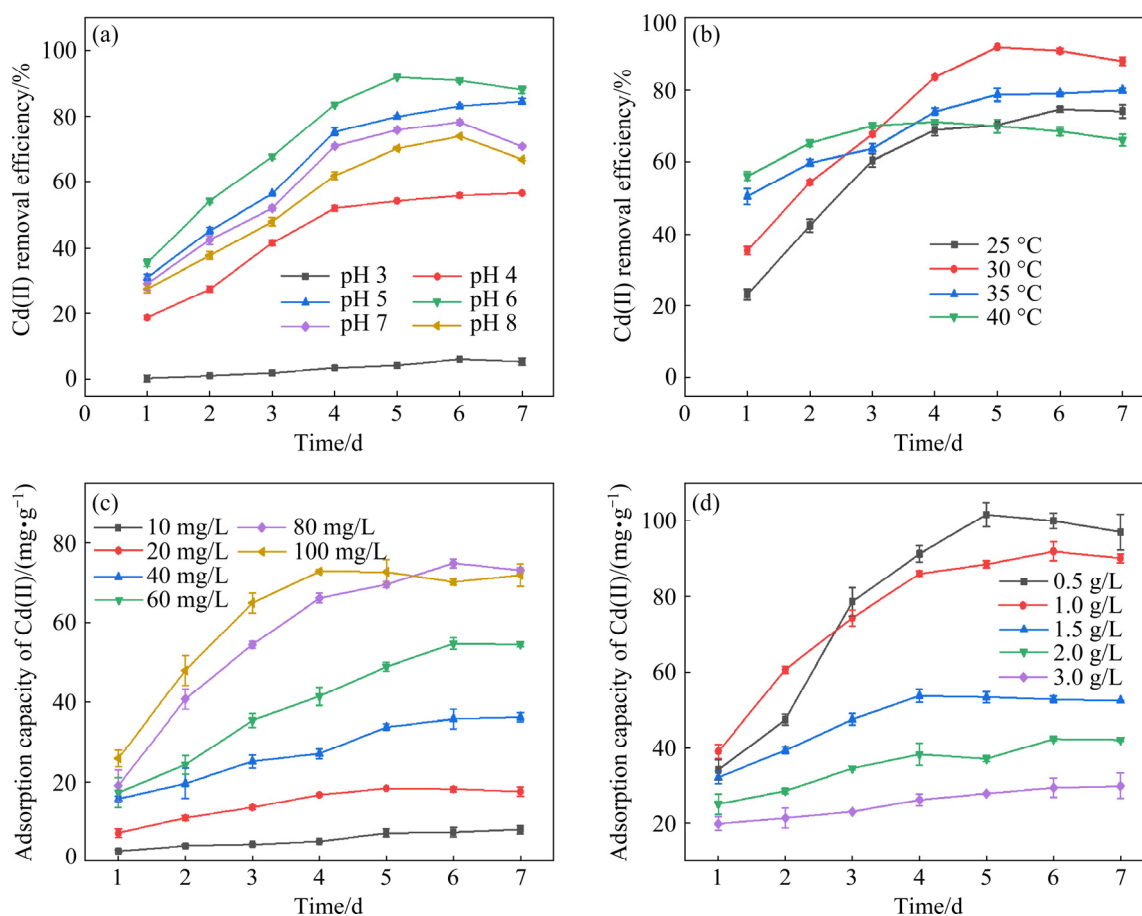


Fig. 1 Effects of varying environmental factors on Cd(II) removal efficiency (a, b) and adsorption capacity of Cd(II) (c, d): (a) pH; (b) Temperature; (c) Initial Cd(II) concentration; (d) Biomass dosage

SATYA et al [17] found that using *Aphanotheca* sp. as a biosorbent achieved a maximum Cd(II) adsorption capacity of 66.80 mg/g at 30 °C, which was significantly lower than the maximum adsorption capacity achieved in the present study (101.58 mg/g). Previous studies have shown that persistent high temperatures damage the structure of the microbial cell membranes [18,29], leading to a slight decrease in the adsorption of HMs. Therefore, the optimum temperature was selected to be 30 °C, which was applied for all subsequent tests.

3.2.3 Effect of initial Cd(II) concentration

The living biomass adsorption capacity with different initial Cd(II) concentrations (10–100 mg/L) is shown in Fig. 1(c). The maximum adsorption capacity of Cd(II) was 74.93 mg/g with an initial Cd(II) concentration of 80 mg/L, which was far higher than that of 7.23 mg/g with an initial Cd(II) concentration of 10 mg/L. It can be observed that, when the adsorption time and dosage of biomass remained constant, the adsorption capacity was

improved with increasing the initial Cd(II) concentration. This might be due to the increase in initial Cd(II) concentration causing a higher driving force between the solution and the surface of biomass to overcome the mass transfer resistance, as reported previously by ARIVALAGAN et al [28]. However, the adsorption capacity of living biomass was reduced after exposure to an initial Cd(II) concentration of 100 mg/L for 5 d. It might be speculated that the saturation of the active adsorption sites on biosorbent surface occurred, making them less available for metal binding [17,30].

3.2.4 Effect of biomass dosage

Figure 1(d) shows the effect of varying living biomass dosages (0.5–3.0 g/L) on the adsorption capacity of Cd(II), with removal performed at pH 6.0 and 30 °C. Results revealed that the living biomass adsorption capacity decreased progressively with increasing biomass dosages. The adsorption capacity of living biomass varied from (101.58±3.17) mg/g (for 0.5 g/L sorbent) to (28.01±0.33) mg/g (for 3.0 g/L sorbent) with a

contact time of 120 h. A recent study performed using *Mucoromycote* sp. XLC at a biomass dosage of 0.5 g/L showed that the maximum adsorption capacities of Cd(II) and Ni(II) were 79.65 and 51.26 mg/g, respectively [31]. This could be attributed to a partial aggregation of biomass at higher dosages, resulting in less favorable sites being available for the removal of Cd(II) [17,32]. In addition, after the 5th day, the adsorption capacity of Cd(II) did not continue to increase consistently, with a slight reduction observed at a 0.5 g/L biomass dosage. Overall, the optimal removal effect was observed at 1.0 g/L Cd(II). Therefore, the optimum living biomass dosage of 1.0 g/L was applied for all subsequent experiments.

3.2.5 Biosorption performance of living and autoclaved biomasses

A comparison of the Cd(II) biosorption performance of living and autoclaved biomasses over 120 h is shown in Fig. 2. The results show that with varying environmental conditions (pH, temperature, initial Cd(II) concentration, and

biomass dosage), the Cd(II) removal efficiency by living biomass (91.97%) was evidently higher than that of autoclaved biomass (79.54%). For both living and autoclaved biomasses, the Cd(II) removal efficiency increased when the pH was increased from 3 to 6, then decreased with further increase in pH. The effect of varying temperature conditions followed a similar pattern, with the maximum Cd(II) removal efficiency obtained at 30 °C, then decreasing from 35 to 40 °C. These results are in line with the previously reported findings of MOHAPATRA et al [18]. The reduced adsorption capacity of autoclaved cells may be because the autoclaving process destroys the cell membrane structure of biomass, reducing the number of available adsorption sites and inhibiting intracellular Cd(II) bioaccumulation [13]. Finally, results showed that the optimal conditions for adsorption using autoclaved biomass were pH 6, 30 °C, initial Cd(II) concentration of 20 mg/L and biomass dose of 1.0 g/L, which were consistent to the optimal conditions established using living biomass.

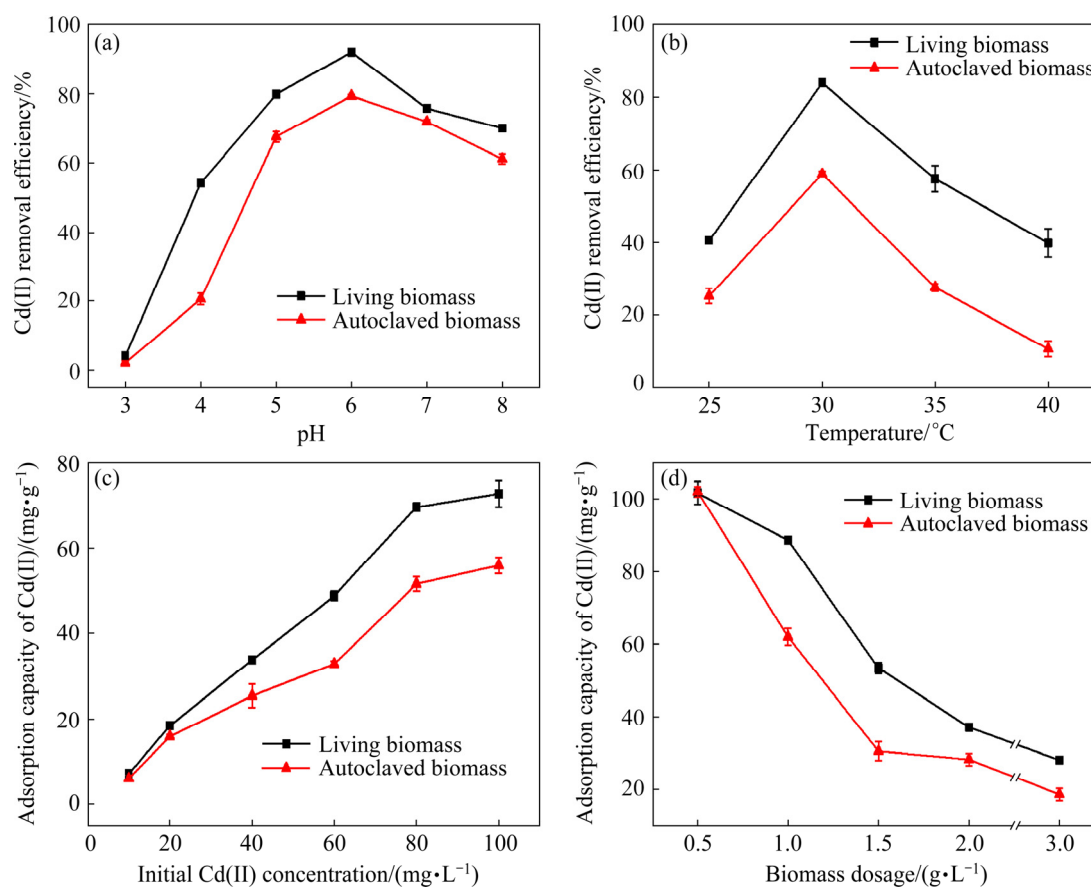


Fig. 2 Comparison of Cd(II) removal efficiencies and adsorption capacity of living and autoclaved biomass after exposure to Cd(II) for 120 h under varying environmental conditions: (a) pH; (b) Temperature; (c) Initial Cd(II) concentration; (d) Biomass dosage

3.3 Adsorption isotherms

The obtained data were fitted using Langmuir and Freundlich adsorption isotherm models (Figs. 3(a) and (b), respectively), with the corresponding parameters shown in Table 1. The Langmuir isotherm was used to identify the maximum theoretical metal uptake values based on the principle of monolayer biosorption [33]. In contrast, the Freundlich isotherm was used to explain the biosorption of metal ions onto heterogeneous surfaces [10]. The coefficient determinant (R^2) values obtained from the Langmuir and Freundlich fitting curves were 0.992 and 0.981 for living biomass and 0.988 and 0.982 for autoclaved

biomass, respectively. These results show that Cd(II) biosorption by both living and autoclaved biomass was more suitably fitted using the Langmuir model than the Freundlich model, indicating that Cd(II) and the biosorbent interacted via a monolayer biosorption mechanism [18]. Furthermore, the n values of living biomass and autoclaved biomass were 1.1312 and 1.1325, respectively, with both values being greater than 1.0, implying that Cd(II) was favorably adsorbed by both living and autoclaved biomasses [13,18]. It is noted that similar results have been reported previously with the biosorption of Cd(II) by live and dead *Bacillus cereus* RC-1 [13].

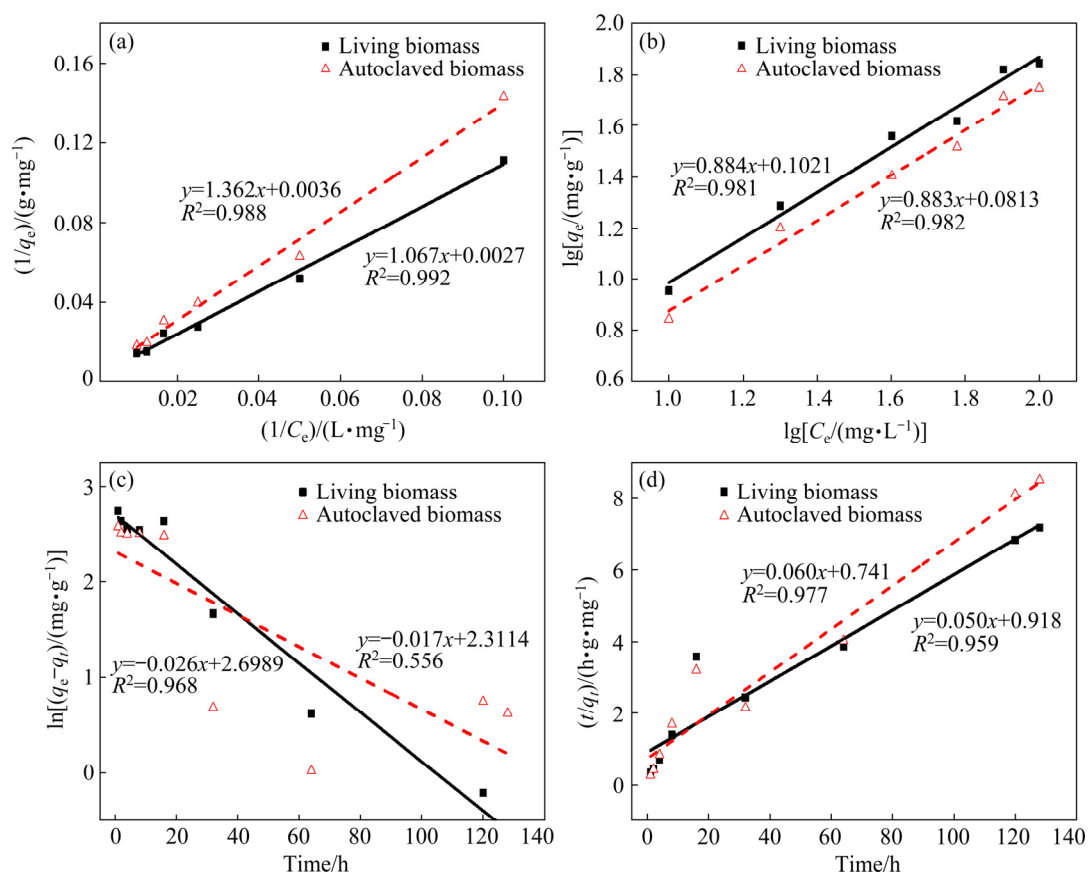


Fig. 3 Adsorption isotherms and linear adsorption kinetics fitting with living and autoclaved biomasses: (a) Langmuir model; (b) Freundlich model; (c) Pseudo-first-order kinetic model; (d) Pseudo-second-order kinetic model

Table 1 Parameters of Langmuir and Freundlich adsorption isotherm models

Biomass	Langmuir model ($\frac{1}{q_e} = \frac{1}{C_e} \cdot \frac{1}{q_m K_L} + \frac{1}{q_m}$)			Freundlich model ($\lg q_e = \lg K_f + \frac{\lg C_e}{n}$)		
	$q_m/(\text{mg} \cdot \text{g}^{-1})$	$K_L/(\text{mg} \cdot \text{g}^{-1})$	R^2	$K_f/(\text{mg}^{1-n} \cdot \text{L}^n \cdot \text{g}^{-1})$	n	R^2
Living	370.37	0.0025	0.992	1.26	1.1312	0.981
Autoclaved	277.78	0.0026	0.988	1.21	1.1325	0.982

q_e is equilibrium adsorption capacity, q_m is instant adsorption capacity, K_L is Langmuir adsorption equilibrium constant, K_f is Freundlich adsorption equilibrium constant, and n is empirical parameter related to adsorption strength

3.4 Adsorption kinetics

To explain the adsorption process dynamics for the removal of 20 mg/L Cd(II), pseudo-first-order and pseudo-second-order kinetic models were applied to fitting the adsorption data (Figs. 3(c) and (d)), with the rate constant values provided in Table 2. According to the corresponding correlation coefficient (R^2) values, Cd(II) removal by living biomass fitting using the pseudo-first-order kinetic model ($R^2=0.968$) and the pseudo-second-order model ($R^2=0.959$) was not much different, indicating that the effect of biosorption by living biomass depended on the number of available binding sites and also the involved chemical adsorption [33]. In contrast, the autoclaved biomass fitted better for pseudo-second-order kinetic model ($R^2=0.977$) than the pseudo-first-order model ($R^2=0.556$), indicating that the functional groups on the autoclaved biomass surface may be involved in the kinetics of the rate-limiting step during Cd(II) biosorption [34]. Consequently, the formation of chemical bonds between Cd(II) and the biomass functional groups is considered to be the dominant mechanism [35]. Furthermore, the pseudo-second-order rate constant (k_2) for autoclaved biomass (0.005 g/(mg·min)) was higher than that for living biomass (0.003 g/(mg·min)), indicating that the adsorption of Cd(II) by autoclaved biomass occurred more rapidly than by living biomass, which was consistent with the previously reported findings for Cd(II) biosorption using *Pseudomonas* sp. strain 375 [3].

3.5 Removal efficiency of multiple co-occurring HMs by living and autoclaved biomasses

The efficiency of adsorption of multiple co-occurring HMs by living and autoclaved biosorbents in supplemented wastewater is shown in Fig. S4, with the One-way ANOVA results shown in Table S2. After 5 d of biosorption, the Cd(II) removal efficiencies were 69.52 % and 53.51% for living and autoclaved biomasses, respectively,

which were lower than the equivalent efficiencies established in the batch study (91.97%), probably due to the co-occurring metal ions competing for the available adsorption sites [9]. However, Pb(II), Cu(II) and Zn(II) were found to be efficiently removed by living biomass with concentrations reduced by 99.96%, 94.63% and 81.08%, respectively. Furthermore, the living biomass consistently achieved higher HM biosorption capacities than autoclaved biomass. Although living biomass had higher biosorption capacities for Pb(II), Cu(II) and Zn(II), no significant difference was observed between the removal efficiencies of Cd(II) and Zn(II) ($p>0.05$). However, the removal efficiencies of Pb(II), Cu(II) and Mn(II) exhibited significant differences to Cd(II) ($p<0.05$), which may imply that Pb(II), Cu(II) and Mn(II) had a small influence on the biosorption of Cd(II). With the autoclaved biomass, the HM removal efficiencies were not high and no significant differences were observed between the removal efficiency of Cd(II) and that of Zn(II) or Cu(II) ($p>0.05$). However, Pb(II) and Mn(II) exhibited a significant difference with Cd(II) ($p<0.05$). A similar study by XU et al [3] used *Pseudomonas* sp. strain 375 to treat raw wastewater containing HMs such as Cd(II), Pb(II), Cu(II), Zn(II), Co(II) and Mn(II), finding that Pb(II) and Cu(II) were efficiently removed with a high removal rate. Therefore, living biomass is a promising biosorbent for use in the bioremediation of HM contaminated water.

3.6 Characterization of Cd(II) immobilization mechanism

3.6.1 Cd(II) immobilization pathways

After the exposure of 20 mg/L biomass to Cd(II) for 120 h, the Cd(II) immobilization pathways were investigated by analyzing the Cd(II) content of loosely, tightly and intracellularly bound fractions, as shown in Fig. S5. The percentages of Cd(II) immobilized in the loosely, tightly and intracellularly

Table 2 Constants of pseudo-first-order and pseudo-second-order kinetic models for living and autoclaved biomasses under optimized conditions

Biomass	$q_{\text{exp}}/(\text{mg}\cdot\text{g}^{-1})$	Pseudo-first-order model $\ln(q_e - q_t) = \ln q_e - k_1 t$			Pseudo-second-order model $\frac{t}{q_t} = \frac{t}{q_e} + \frac{1}{k_2 q_e^2}$		
		k_1/min^{-1}	$q_e/(\text{mg}\cdot\text{g}^{-1})$	R^2	$k_2/(\text{g}\cdot\text{mg}^{-1}\cdot\text{min}^{-1})$	$q_e/(\text{mg}\cdot\text{g}^{-1})$	R^2
Living	18.39	0.026	14.86	0.968	0.003	20.00	0.959
Autoclaved	16.89	0.017	10.09	0.556	0.005	16.67	0.977

bound fractions were $(16.50\pm 4.58)\%$, $(74.90\pm 3.87)\%$ and $(4.50\pm 1.02)\%$ in living biomass, and $(32.77\pm 0.81)\%$, $(64.95\pm 7.16)\%$ and $(1.18\pm 0.39)\%$ in autoclaved biomass, respectively. Overall, Cd(II) was mainly adsorbed in the loosely and tightly bound layers of the bacterial surface. Previous studies [13] have indicated that higher surface adsorption of metals by bacteria, occurs as protection barrier, reducing the concentration of metals in the cytoplasm, serving effectively as a bacterial detoxification mechanism. CHAKRAVARTY and BANERJEE [36] also reported that the biosorption of Cd(II) on *Acidiphilium symbioticum* H8 cell membranes occurred via chemical adsorption (complexes formation), exchange of cations and electrostatic interaction mechanisms.

3.6.2 SEM–EDS results

The surface morphology and elemental composition of the living biomass before (Figs. 4(a) and (b)) and after (Figs. 4(c) and (d)) Cd(II) adsorption were measured by SEM–EDS. The cell surface of the living biomass was initially smooth and tightly arranged with regular shapes, mostly oval or spherical in Fig. 4(a). After Cd(II) biosorption, the morphology of the living biomass changed significantly (Fig. 4(c)), developing a loosely arranged cell surface. EDS spectra analysis was used to establish the elemental composition of the cell surface, about 0.33% Cd(II) was present on the surface of living biomass after biosorption (Fig. 4(d)) compared with pre-biosorption (Fig. 4(b)). In contrast, cell rupture was observed in the autoclaved biomass, or smack holes were present on the surface of in-tact cells, which were mostly short rod-shaped cells (Fig. 4(e)). After biosorption the rod-shaped autoclaved cells were less abundant and more spheres appeared, with granular substances on their surface (Fig. 4(g)). Meanwhile, the EDS spectrum obtained for autoclaved biomass after Cd(II) biosorption confirmed the presence of Cd(II) on the cell surfaces (Fig. 4(h)).

HUANG et al [13] reported that changes in cell surface morphology may occur due to a reduction in mechanical force caused by the interaction between surface functional groups and metallic ions. In addition, MOHAPATRA et al [18] also observed similar results for the surface of *Pseudomonas* cells after Pb(II) biosorption, with Pb(II) appearing as electron-dense bright

precipitates on the cell surface, speculated to be Pb(OH)₂ complex formation. Furthermore, the contents of carbon, phosphorous, and sulfur on the surface of living and autoclaved biomasses increased, while the contents of nitrogen and oxygen decreased. This contributes to the capacity that many microorganisms have to adapt to environmental changes via surface modification [33] such as the P- and S-containing functional groups involved in HM adsorption. For example, changes in the structure of cell membrane phospholipids lead to an increase in the P content, while amide groups were consumed during the adsorption process, resulting in a decrease in the contents of N and O elements.

3.6.3 FTIR spectra

The FTIR spectra of living and autoclaved biomasses before and after exposure to Cd(II) are shown in Fig. 5(a), with the peaks related to functional groups listed in Table S3. There were a variety of anionic ligands identified on the cell surface of living biomass, such as hydroxyl ($3420\text{--}3240\text{ cm}^{-1}$), amine ($1685\text{--}1350\text{ cm}^{-1}$), thiocarbonyl ($1200\text{--}1020\text{ cm}^{-1}$), and phosphate groups ($3420\text{--}3240\text{ cm}^{-1}$). For the autoclaved biomass, the position of some peaks slightly shifted due to differences in the transmittance of functional groups as compared to living biomass, while other characteristics remained consistent with the living biomass. In particular, the peak at around 625 cm^{-1} in the living biomass spectrum fingerprint, attributed to amines and nitro groups, was not observed in the autoclaved biomass, indicating that some structural components of cells were destroyed by high temperature treatment [37].

The peak at around 3299 cm^{-1} in living biomass was attributed to the overlapping stretching vibrations of —OH on alcohols and —NH₂ on amines [33,38], shifting to 3416 cm^{-1} and widening after Cd(II) biosorption. Three strong peaks were observed at $1670\text{--}1390\text{ cm}^{-1}$, which were attributed to the vibration of C=O, —NH₂ and —CN bands in amide I, II and III, respectively [13,27,39,40]. The peak observed at 1237 cm^{-1} was attributed to P=O symmetric stretching, while the peak at 1078 cm^{-1} was attributed to C=S and S=O, and the peak at 700 cm^{-1} can be attributed to various cell surface functional groups containing S and P [17,41], indicating the participation of phospholipids, proteins and polysaccharides. Analysis of the

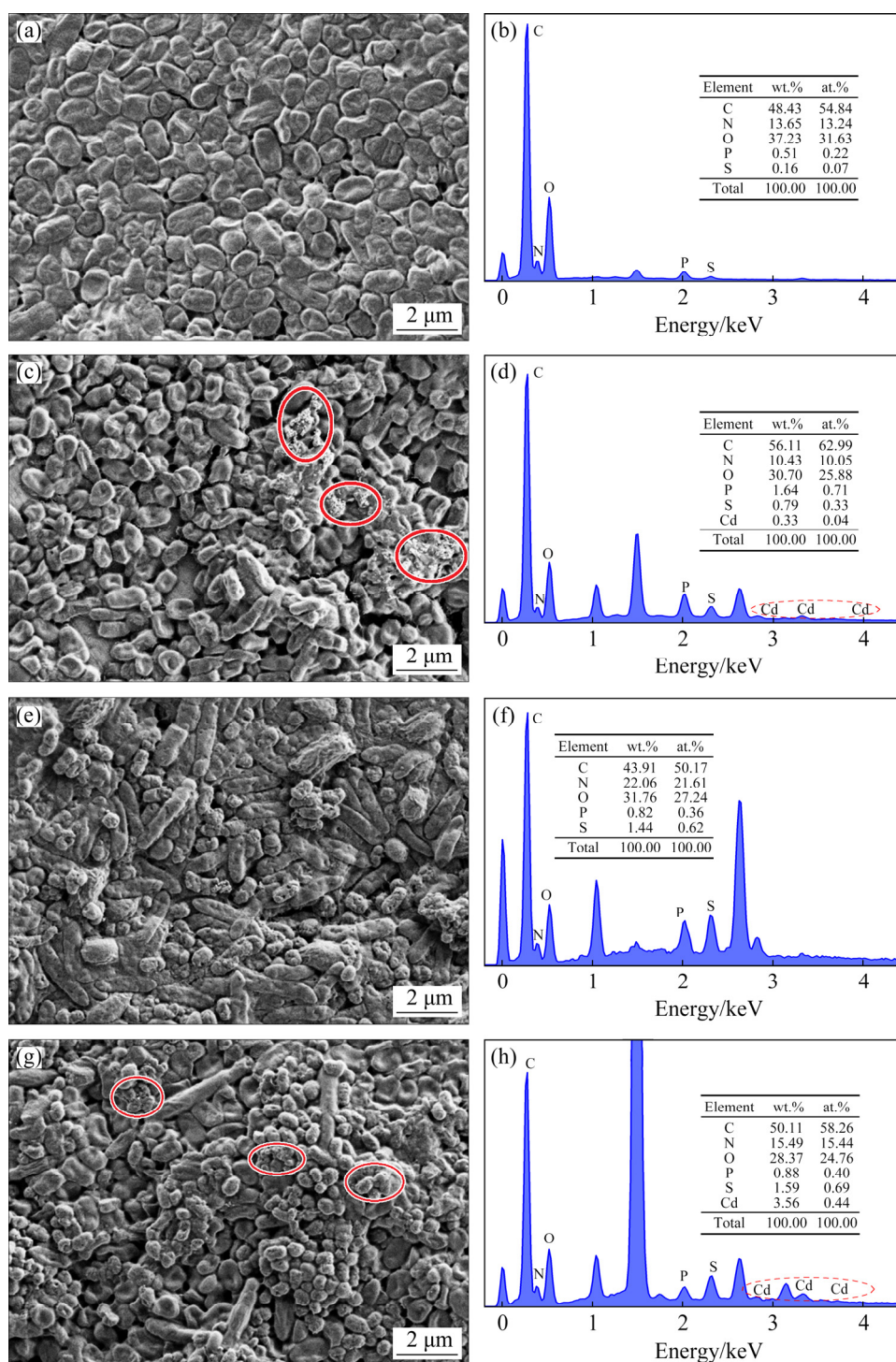


Fig. 4 SEM–EDS analysis results of living and autoclaved biomasses before and after biosorption of Cd(II): (a, b) Living biomass without Cd(II); (c, d) Living biomass with Cd(II); (e, f) Autoclaved biomass without Cd(II); (g, h) Autoclaved biomass with Cd(II)

shift in transmittance peak position and shape revealed that these functional groups participated in Cd(II) biosorption process, which was consistent with the EDS analysis results. Overall, this suggests that amine, hydroxyl, thiocarbonyl, nitro, and phosphoric acid groups participate in the Cd(II)

adsorption process.

3.6.4 XRD patterns

The XRD patterns generated for the living and autoclaved biomasses before and after being exposed to Cd(II) are shown in Fig. 5(b). The main diffraction peaks of Cd(OH)₂ occurred at 2θ values

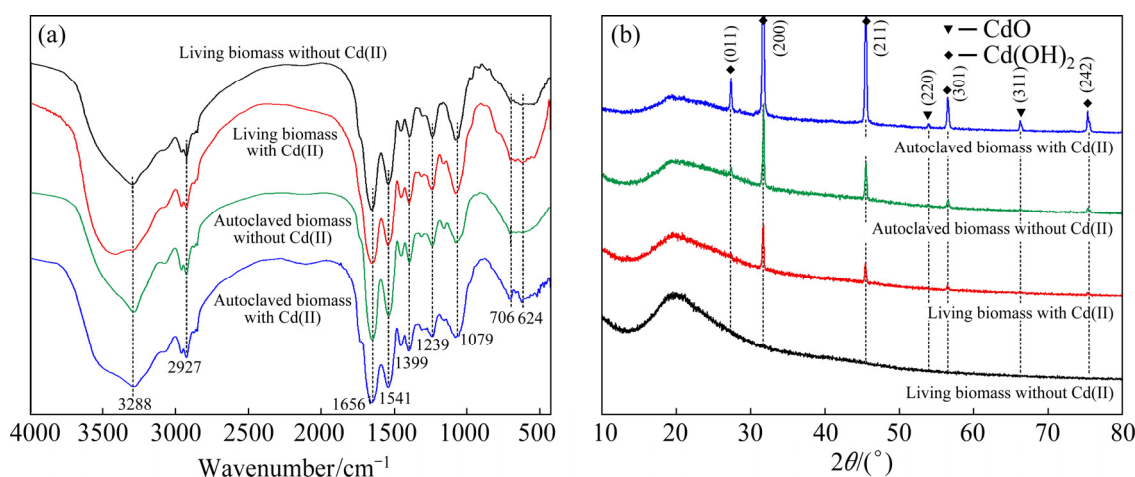


Fig. 5 FTIR spectra (a) and XRD patterns (b) of living and autoclaved biomasses before and after Cd(II) exposure

of 27.4°, 31.5°, 50°, 56.2°, and 75.2° and were related to the diffractions planes of (011), (200), (211), (301), and (242), respectively [42]. In addition, the diffraction peaks of crystalline CdO occurred at 2θ values of 55.3° and 65.9°, corresponding to the crystal planes (220) and (311), respectively [43]. XRD peaks of living biomass exhibited less intensity prior to Cd(II) biosorption, indicating that the amorphous nature of the living biomass occurred mainly due to the presence of lipids, proteins, polysaccharides and fatty acids in the bacterial cell wall [18]. However, significant diffraction peaks appeared at 2θ values of 27.4°, 31.5°, 50°, and 56.2° after biosorption, indicating that the Cd(OH)₂ crystal structure was formed after exposure to Cd(II). With the autoclaved biomass, there was no significant change in the diffraction pattern before and after biosorption, indicating that the chemical structure of the autoclaved biomass remained relatively stable. However, new sharp diffraction peaks appeared at 2θ values of 55.3° and 65.9°, indicating that crystalline CdO was obtained.

3.7 Bacterial community structure and functional prediction

3.7.1 Bacterial composition and phylogenetic tree

Figure 6 shows the bacterial compositions of the initial biomass and the living biomass after being exposed to 20 mg/L Cd(II) for 144 h. The dominant genera in the initial biomass sample were *unclassified_f_Enterobacteriaceae* (63.95%), *Alcaligenes* (18.49%), *Tissierella* (9.07%), *unclassified_f_Peptostreptococcaceae* (5.66%), and *Terrisporobacter* (1.66%). After exposure to

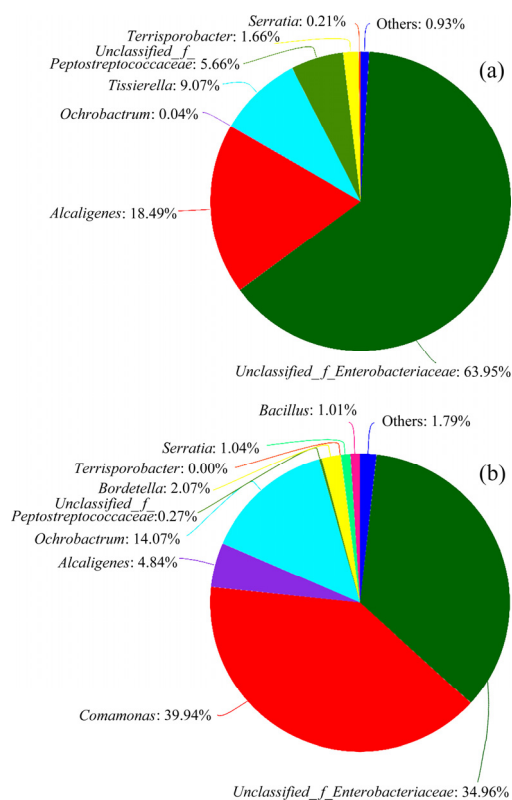


Fig. 6 Composition of bacterial communities at genus level in initial biomass (a) and living biomass (b) exposed to 20 mg/L Cd(II) after 144 h

20 mg/L Cd(II), the dominant genera were *Comamonas* (39.94%), *unclassified_f_Enterobacteriaceae* (34.96%), *Ochrobactrum* (14.07%), *Alcaligenes* (4.84%), *Ochrobactrum* (14.07%), *Bordetella* (2.07%), *Serratia* (1.04%), and *Bacillus* (1.01%). These findings show that the microbial community structure changed significantly, with *Comamonas*, *Bordetella* and *Bacillus* emerging following Cd(II) exposure, while the proportions of

Ochrobactrum and *Serratia* increased from <1% in the initial biomass to dominant component after Cd(II) exposure. For example, the proportional abundances of *Ochrobactrum* and *Serratia* after Cd(II) exposure increased from 0.04% and 0.21% to 14.07% and 1.04%, respectively. It has been reported that *Comamonas* sp. exhibit a high resistance and strong accumulation capacity for Cd(II), with the ability to biosynthesize intracellular Cd-nanoparticles [16]. *Bordetella petrii* have been shown to remove high concentrations of Cd(II) and Ni(II) from leachate, exhibiting resistance to 900 mg/L Cd(II) and 1100 mg/L Ni(II) [12]. Furthermore, it has been reported that *Bacillus* sp. has a maximum Cd(II) biosorption capacity of 163.93 mg/g at pH 5 [15]. *Ochrobactrum* sp. has been reported to grow well in the presence of high concentrations of Cu(II) (4.34 mmol/L) and Cd(II) (1.52 mmol/L) [44], which has also been shown with other *Ochrobactrum* strains [45,46]. In addition, it has been found that *Serratia* biofilms play an active role in Cd(II) adsorption [47]. Therefore, these bacterial genera all exhibited good Cd(II) tolerance in the present study. In contrast, the proportions of *Unclassified_f_Enterobacteriaceae*, *Unclassified_f_Peptostreptococcaceae*, and *Alcaligenes* decreased distinctly after Cd(II) exposure, while *Tissierella* and *Terrisporobacter* disappeared completely, indicating that these bacterial genera were adversely affected by Cd(II) or eliminated from the bacterial community.

Phylogenetic tree was constructed at the genus level (Fig. 7), showing that after exposure to Cd(II), all the genera could be grouped into the

phyla Proteobacteria and Firmicutes, with respective abundance ratios of 96.92% and 1.01%. It has been reported that Proteobacteria is the dominant phylum in soils contaminated with Cd(II) for a long period of time [48]. Therefore, Proteobacteria plays an obviously important role in the biosorption of Cd(II). *Serratia* and *unclassified_f_Enterobacteriaceae* were closely related, being located on the same small branch of the phylogenetic tree. Similarly, *Alcaligenes*, *Bordetella*, and *Comamonas* exhibited a close genetic relationship. These 5 genera and *Ochrobactrum* all belong to Proteobacteria phylum. In contrast, *Unclassified_f_Peptostreptococcaceae* and *Terrisporobacter* exhibit a high degree of homology and a close genetic relationship, belonging to the phylum Firmicutes along with *Tissierella* and *Bacillus*.

The relative proportions of reads for different genera in the phylogenetic tree showed some differences for the initial biomass and the living biomass following exposure to 20 mg/L Cd(II). Results showed that a high degree of phylogenetic evolution occurred in *Comamonas*, *Bordetella*, *Bacillus*, and *Ochrobactrum* due to exposure to 20 mg/L Cd(II), resulting in increased abundances. However, the reads of *unclassified_f_Enterobacteriaceae*, *unclassified_f_Peptostreptococcaceae*, *Alcaligenes*, *Tissierella*, and *Terrisporobacter* were all reduced. Similar results have been reported in a study on microbial community treatment of soil under Cd(II) stress conditions, which speculated that Cd(II) stress caused systematic evolution of the microbial community in soil [49].

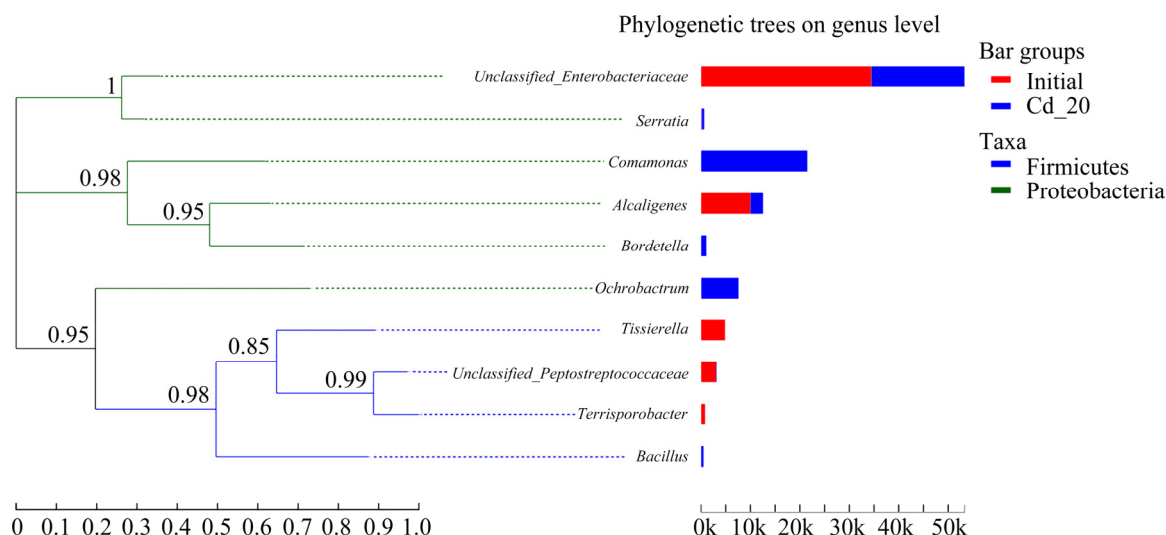


Fig. 7 Phylogenetic tree based on 16S rDNA sequences from microbial community of living biomass

3.7.2 Functional prediction of living biomass community

The bacterial community function in the biomass was predicted using PICRUSt, which revealed the change in bacterial community function according to COG database screening (Fig. 8(a)). The COG type function description E defined as “Amino acid transport and metabolism” had the highest abundance (9.57%) in the initial biomass, reducing to 9.39% after exposure to 20 mg/L Cd(II), which might be related to Cd(II) biosorption with amine groups. The abundance of function S defined as “Function unknown”

increased from 9.47% to 11.56% after Cd(II) exposure, indicating that there exist a larger number of unknown functions in living bacterial biomass that need to be ascertained [23]. Genes, which exhibited an increase in abundance by at least 0.5% following Cd(II) adsorption, were found to be related to transcription, inorganic ion transport and metabolism, signal transduction mechanisms, lipid transport and metabolism, and secondary metabolite biosynthesis, transport and catabolism. Based on these findings, it may be speculated that Cd(II) affected the transformation and transport of materials across the cell membrane.

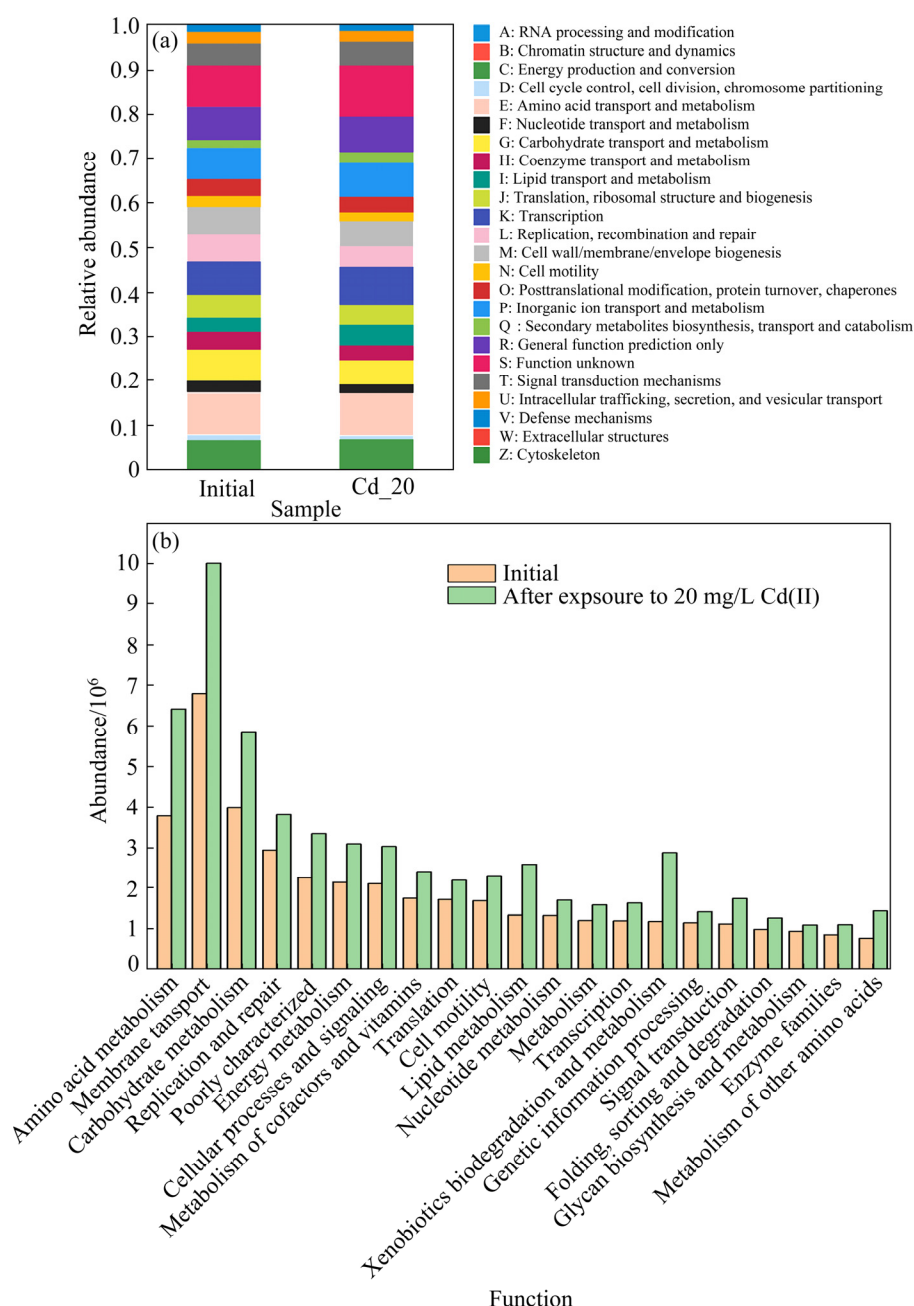


Fig. 8 Functional prediction of living biomass based on COG and KEGG analysis: (a) COG classification statistics before and after Cd(II) biosorption; (b) Level 2 pathway classification statistics based on KEGG database

Based on the KEGG database, the bacterial functional prediction was divided into 6 types of level 1 pathway, including 39 types of level 2 pathway, with the classification statistics for the level 2 pathways shown in Fig. 8(b). The gene abundances of 5 typical functions in the level 2 pathway changed significantly, relating to amino acid metabolism, replication and repair, lipid metabolism, xenobiotics biodegradation and metabolism, and metabolism of other amino acids. These results are consistent with the COG analysis results, inferring that a variety of amino acids and phospholipids on the cell membrane enhanced the biosorption and metabolism of Cd(II) by living biomass.

4 Conclusions

(1) Multiple bacteria were successfully enriched from polymetallic mine soil for the biosorption of Cd(II). Living biomass exhibited higher Cd(II) removal efficiency (91.97%) than autoclaved biomass (79.54%) under optimum conditions (pH 6.0, 30 °C, 20 mg/L initial Cd(II) concentration, and 1 g/L biomass dosage).

(2) The isotherms and kinetics of living biomass conformed to the Langmuir isotherm model and pseudo-first-order kinetic model, respectively. SEM-EDS, FTIR, and XRD analyses confirmed amine groups, hydroxyl groups and phosphoric acid participated in the Cd(II) adsorption process, while crystalline Cd(OH)₂ and CdO were formed.

(3) After exposure to 20 mg/L Cd(II), the dominant genera were *Comamonas* (39.94%), *Unclassified_f_Enterobacteriaceae* (34.96%), *Alcaligenes* (4.84%), *Ochrobactrum* (14.07%), *Bordetella* (2.07%), *Serratia* (1.04%), and *Bacillus* (1.01%). COG and KEGG function prediction found that the abundances of some metabolic genes changed significantly.

Supplementary Materials

Supplementary Materials in this paper can be found at: http://www.yzxbcn.com/download/19-p3404-2021-0938-Supplementary_Materials.pdf

Acknowledgments

This research was supported by the National

Natural Science Foundation of China (No. 52170164), the Open Project of Key Laboratory of Environmental Biotechnology, CAS (No. kf2018001), and the Scientific Research Foundation for Returned Scholars at the University of South China (No. 2018XQD25). The authors thank the Lab staff members Ying-jiu LIU and Ping-li CAI for guidance on analytical instruments.

References

- [1] FENG Ning-chuan, FAN Wei, ZHU Mei-lin, GUO Xue-yi. Adsorption of Cd²⁺ in aqueous solutions using KMnO₄-modified activated carbon derived from *Astragalus* residue [J]. Transactions of Nonferrous Metals Society of China, 2018, 28: 794–801.
- [2] YAN Hong-jie, ZHANG He-yang, SHI Ya-jun, ZHOU Ping, LI Huan, WU Dong-ling, LIU Liu. Simulation on release of heavy metals Cd and Pb in sediments [J]. Transactions of Nonferrous Metals Society of China, 2021, 31: 277–287.
- [3] XU Shao-zu, XING Yong-hui, LIU Song, HAO Xiu-li, CHEN Wen-li, HUANG Qiao-yun. Characterization of Cd²⁺ biosorption by *Pseudomonas* sp. strain 375, a novel biosorbent isolated from soil polluted with heavy metals in Southern China [J]. Chemosphere, 2020, 240: 124893.
- [4] DAI Shu-juan, WEI De-zhou, ZHOU Dong-qin, JIA Chun-yun, WANG Yu-juan, LIU Wen-gang. Removing cadmium from electroplating wastewater by waste *Saccharomyces cerevisiae* [J]. Transactions of Nonferrous Metals Society of China, 2008, 18: 1008–1013.
- [5] BUAH W K, DANKWAH J R. Sorption of heavy metals from mine wastewater by activated carbons prepared from coconut husk [J]. Ghana Mining Journal, 2016, 16: 36–41.
- [6] State Environmental Protection Administration of China. GB 8978—996, Integrated wastewater discharge standard [S]. Beijing: China Environmental Science Press, 1996: 272–289. (in Chinese)
- [7] SIS H, UYSAL T. Removal of heavy metal ions from aqueous medium using Kuluncak (Malatya) vermiculites and effect of precipitation on removal [J]. Applied Clay Science, 2014, 95: 1–8.
- [8] ZEWAİL T M, YOUSEF N S. Kinetic study of heavy metal ions removal by ion exchange in batch conical air spouted bed [J]. Alexandria Engineering Journal, 2015, 54: 83–90.
- [9] CHENG Jin-feng, YIN Wen-ke, CHANG Zhao-yang, LUNDHOLM N, JIANG Zai-min. Biosorption capacity and kinetics of cadmium(II) on live and dead *Chlorella vulgaris* [J]. Journal of Applied Phycology, 2017, 29: 211–221.
- [10] BULGARIU L, LUPEA M, BULGARIU D, RUSU C, MACOVEANU M. Equilibrium study of Pb(II) and Cd(II) biosorption from aqueous solution on marine green algae biomass [J]. Environmental Engineering and Management Journal, 2013, 12: 183–190.
- [11] XUE Chao, QI Pei-shi, LI Meng-sha, LIU Cheng-bin. Characterization and sorptivity of the *Plesiomonas shigelloides* strain and its potential use to remove Cd²⁺ from wastewater [J]. Water, 2016, 9: 45.

- [12] SANUTH H A, ADEKANMBI A O. Biosorption of heavy metals in dumpsite leachate by metal-resistant bacteria isolated from Abule-egba dumpsite, Lagos State, Nigeria [J]. *Microbiology Research Journal International*, 2016, 17: 1–8.
- [13] HUANG Fei, DANG Zhi, GUO Chu-ling, LU Gui-ning, GU R R, LIU Hong-juan, ZHANG Hui. Biosorption of Cd(II) by live and dead cells of *Bacillus cereus* RC-1 isolated from cadmium-contaminated soil [J]. *Colloids and Surfaces B: Biointerfaces*, 2013, 107: 11–18.
- [14] PARITOSH P, ARPIT S, DWEIPAYAN G, BALDEV P, MEENU S. Optimization of cadmium and lead biosorption onto marine *Vibrio alginolyticus* PBR1 employing a box-behken design [J]. *Chemical Engineering Journal Advances*, 2020, 4: 100043.
- [15] LONG Jian-you, YU Ming-xia, XU Huai-hao, HUANG Shuang-qiu, WANG Zhu, ZHANG Xu-xiang. Characterization of cadmium biosorption by inactive biomass of two cadmium-tolerant endophytic bacteria *Microbacterium* sp. D2-2 and *Bacillus* sp. C9-3 [J]. *Ecotoxicology (London, England)*, 2021, 30: 1419–1428.
- [16] SHI Zun-ji, QI Xiao-li, ZENG Xin-an, LU Yu-jing, ZHOU Jin-lin, CUI Ke-hui, ZHANG Li-min. A newly isolated bacterium *Comamonas* sp. XL8 alleviates the toxicity of cadmium exposure in rice seedlings by accumulating cadmium [J]. *Journal of Hazardous Materials*, 2021, 403: 123824.
- [17] SATYA A, HARIMAWAN A, HARYANI G S, JOHIR M A H, VIGNESWARAN S, NGO H H, SETIADI T. Batch study of cadmium biosorption by carbon dioxide enriched *Aphanotheca* sp. dried biomass [J]. *Water*, 2020, 12: 264.
- [18] MOHAPATRA R K, PARHI P K, PANDEY S, BINDHANI B K, THATOI H, PANDA C R. Active and passive biosorption of Pb(II) using live and dead biomass of marine bacterium *Bacillus xiamenensis* PBRPSD202: Kinetics and isotherm studies [J]. *Journal of Environmental Management*, 2019, 247: 121–134.
- [19] MAGYAR M, MEZZETTI A, SIPKA G, ZHU Qing-jun, HAN Guang-ye, LAMBREV P, LEIBL W, SHEN Jian-ren, GARAB G. Light-induced conformational changes in Photosystem II core complexes revealed by rapid-scan Fourier transform infrared spectroscopy [J]. *Biochimica et Biophysica Acta: Bioenergetics*, 2018, 1859: e107.
- [20] ZENG Tao-tao, RENE E R, ZHANG Shi-qi, LENS P N L. Removal of selenate and cadmium by anaerobic granular sludge: EPS characterization and microbial community analysis [J]. *Process Safety and Environmental Protection*, 2019, 126: 150–159.
- [21] ZENG Tao-tao, MO Guan-hai, HU Qing, WANG Guo-hua, LIAO Wei, XIE Shui-bo. Microbial characteristic and bacterial community assessment of sediment sludge upon uranium exposure [J]. *Environmental Pollution*, 2020, 261: 114176.
- [22] SAKAI K, YAMAMOTO Y, IKEUCHI T. Vertebrates originally possess four functional subtypes of G protein-coupled melatonin receptor [J]. *Scientific Reports*, 2019, 9: 9465.
- [23] WANG Xu, LI Da-ping, GAO Ping, GU Wen-zhi, HE Xiao-hong, YANG Wen-yi, ZHONG Tang-wen. Analysis of biosorption and biotransformation mechanism of *Pseudomonas chengduensis* strain MBR under Cd(II) stress from genomic perspective [J]. *Ecotoxicology and Environmental Safety*, 2020, 198: 110655.
- [24] HLIHOR R M, FIGUEIREDO H, TAVARES T, GAVRILESCU M. Biosorption potential of dead and living *Arthrobacter viscosus* biomass in the removal of Cr(VI): Batch and column studies [J]. *Process Safety and Environmental Protection*, 2016, 108: 44–56.
- [25] ADIL J, ANDRÉ D, SAID E H, ZOUHAIR L, ANAS D, ABDELGHANI B, ABDELRAANI Y, MOHAMMED E M, MOHSINE H. Optimization of cadmium ions biosorption by fish scale from aqueous solutions using factorial design analysis and Monte Carlo simulation studies [J]. *Journal of Environmental Chemical Engineering*, 2021, 9: 104727.
- [26] ZHANG Da-wei, ZHANG Ke-jing, HU Xiao-lan, HE Qian-qian, YAN Jin-peng, XUE Ying-wen. Cadmium removal by MgCl₂ modified biochar derived from crayfish shell waste: Batch adsorption, response surface analysis and fixed bed filtration [J]. *Journal of Hazardous Materials*, 2021, 408: 124860.
- [27] QIAO Jun-lian, WANG Lei, FU Xiao-hua, ZHENG Gunag-hong. Comparative study on the Ni²⁺ biosorption capacity and properties of living and dead *Pseudomonas putida* cells [J]. *Iranian Journal of Chemistry & Chemical Engineering: International English Edition*, 2010, 29: 159–167.
- [28] ARIVALAGAN P, SINGARAJ D, HARIDASS V, KALIANNAN T. Removal of cadmium from aqueous solution by batch studies using *Bacillus cereus* [J]. *Ecological Engineering*, 2014, 71: 728–735.
- [29] DAS S, MISHRA J, DAS S K, PANDEY S, RAO D S, CHAKRABORTY A, SUDARSHAN M, DAS N, THATOI H. Investigation on mechanism of Cr(VI) reduction and removal by *Bacillus amyloliquefaciens*, a novel chromate tolerant bacterium isolated from chromite mine soil [J]. *Chemosphere*, 2014, 96: 112–121.
- [30] RONBANCHOB A, PRASERT P. Batch and column studies of biosorption of heavy metals by *Caulerpa lentillifera* [J]. *Bioresource Technology*, 2008, 99: 2766–2777.
- [31] ZHU Wei, XU Xing-jian, XIA Lu, HUANG Qiao-yun, CHEN Wen-li. Comparative analysis of mechanisms of Cd²⁺ and Ni²⁺ biosorption by living and nonliving *Mucoromycote* sp. XLC [J]. *Geomicrobiology Journal*, 2016, 33: 274–282.
- [32] AHMET S, MUSTAFA T. Biosorption of Pb(II) and Cd(II) from aqueous solution using green alga (*Ulva lactuca*) biomass [J]. *Journal of Hazardous Materials*, 2008, 152: 302–308.
- [33] PAUL M L, SAMUEL J, CHANDRASEKARAN N, MUKHERJEE A. Comparative kinetics, equilibrium, thermodynamic and mechanistic studies on biosorption of hexavalent chromium by live and heat killed biomass of *Acinetobacter junii* VITSUKMW2, an indigenous chromite mine isolate [J]. *Chemical Engineering Journal*, 2012, 187: 104–113.
- [34] XU Xing-jian, LI Hai-yan, WANG Quan-ying, LI Dan-dan, HAN Xue-rong, YU Hong-wen. A facile approach for surface alteration of *Pseudomonas putida* I3 by supplying K₂SO₄ into growth medium: Enhanced removal of Pb(II) from aqueous solution [J]. *Bioresource Technology*, 2017, 232: 79–86.
- [35] DING Jing, CHEN Wei-guang, ZHANG Zi-lan, QIN Fan, JIANG Jing, HE An-fei, DANIEL S G. Enhanced removal of cadmium from wastewater with coupled biochar and *Bacillus subtilis* [J]. *Water Science and Technology: A Journal of the*

- International Association on Water Pollution Research, 2021, 83: 2075–2086.
- [36] CHAKRAVARTY R, BANERJEE P C. Mechanism of cadmium binding on the cell wall of an acidophilic bacterium [J]. *Bioresource Technology*, 2012, 108: 176–183.
- [37] AHAD R I A, SYIEM M B, NATH R A. Cd(II) sorption by *Nostoc* sp. JRD1: Kinetic, thermodynamic and isotherm studies [J]. *Environmental Technology & Innovation*, 2021, 21: 101283.
- [38] BASU M, GUHA A K, RAY L. Adsorption of cadmium on cucumber peel: Kinetics, isotherm and co-ion effect [J]. *Indian Chemical Engineer*, 2018, 60: 179–195.
- [39] LI Ding, LI Ru-yi, DING Zhe-xu, RUAN Xiao-fang, LUO Jun, CHEN Jin-yuan, ZHENG Jie, TANG Jian-xin. Discovery of a novel native bacterium of *Providencia* sp. with high biosorption and oxidation ability of manganese for bioleaching of heavy metal contaminated soils [J]. *Chemosphere*, 2020, 241: 125039.
- [40] HUANG Hao-jie, JIA Qing-yun, JING Wei-xin, DAHMS H U, WANG Lan. Screening strains for microbial biosorption technology of cadmium [J]. *Chemosphere*, 2020, 251: 126428.
- [41] ZHANG Zhi-qiang, WANG Pan, ZHANG Jiao, XIA Si-qing. Removal and mechanism of Cu(II) and Cd(II) from aqueous single-metal solutions by a novel biosorbent from waste-activated sludge [J]. *Environmental Science and Pollution Research*, 2014, 21: 10823–10829.
- [42] AKBAR M, EDRIS J, EHSAN M, SHAHRZAD J, FARANAK M. Carrageenan assisted synthesis of morphological diversity of CdO and Cd(OH)₂ with high antibacterial activity [J]. *Materials Research Express*, 2021, 8: 065006.
- [43] RAO H J. Characterization studies on adsorption of lead and cadmium using activated carbon prepared from waste tyres [J]. *Nature Environment and Pollution Technology*, 2021, 20: 561–568.
- [44] CHEN Chen, LEI Wen-rui, LU Min, ZHANG Jia-nan, ZHANG Zhou, LUO Chun-ling, CHEN Ya-hua, HONG Qing, SHEN Zhen-guo. Characterization of Cu(II) and Cd(II) resistance mechanisms in *Sphingobium* sp. PHE-SPH and *Ochrobactrum* sp. PHE-OCH and their potential application in the bioremediation of heavy metal-phenanthrene co-contaminated sites [J]. *Environmental Science and Pollution Research International*, 2016, 23: 6861–6872.
- [45] BABITA S, PRATYOOSH S. A comparative analysis of heavy metal bioaccumulation and functional gene annotation towards multiple metal resistant potential by *Ochrobactrum intermedium* BPS-20 and *Ochrobactrum ciceri* BPS-26 [J]. *Bioresource Technology*, 2021, 320: 124330.
- [46] TAO Qi, LI Jin-xing, LIU Yuan-kun, LUO Ji-peng, XU Qiang, LI Bing, LI Qi-quan, LI Ting-qiang, WANG Chang-quan. *Ochrobactrum intermedium* and saponin assisted phytoremediation of Cd and B[a]P co-contaminated soil by Cd-hyperaccumulator *Sedum alfredii* [J]. *Chemosphere*, 2020, 245: 125547.
- [47] XU Shao-zu, XING Yong-hui, LIU Song, LUO Xue-song, CHEN Wen-li, HUANG Qiao-yun. Co-effect of minerals and Cd(II) promoted the formation of bacterial biofilm and consequently enhanced the sorption of Cd(II) [J]. *Environmental Pollution*, 2020, 258: 113774.
- [48] XU Zhi-nan, YANG Zai-fu, ZHU Tong, SHU Wen-jun, GENG Li-sha. Ecological improvement of antimony and cadmium contaminated soil by earthworm *Eisenia fetida*: Soil enzyme and microorganism diversity [J]. *Chemosphere*, 2021, 273: 129496.
- [49] WANG Xu, GAO Ping, LI Da-ping, LIU Ju, YANG Nuan, GU Wen-zhi, HE Xiao-hong, TANG Wen-zhong. Risk assessment for and microbial community changes in farmland soil contaminated with heavy metals and metalloids [J]. *Ecotoxicology and Environmental Safety*, 2019, 185: 109685.

重金属矿山土壤富集菌去除 Cd(II)的效果、机理及微生物群落

曾涛涛¹, 张晓玲¹, 农海杜¹, 胡青¹, 王亮钦¹, 王爱杰²

1. 南华大学 污染控制与资源化技术湖南省高校重点实验室, 衡阳 421001;

2. 中国科学院 环境生物技术重点实验室, 北京 100085

摘要: 从重金属矿山土壤中富集混合菌用于含镉(Cd(II))废水处理。批量吸附试验结果表明, 适宜的pH、温度、初始Cd(II)浓度和投加量分别为6.0、30℃、20 mg/L和1 g/L。在最适条件下, 活性混合菌对Cd(II)的去除效率(91.97%)高于灭活混合菌(79.54%)。活性混合菌的吸附等温线和动力学过程分别符合Langmuir模型和准一级动力学模型。FTIR结果表明, 胺基、羟基和磷酸在Cd(II)的吸附中发挥重要作用; XRD结果表明, 反应后存在Cd(OH)₂和CdO晶体。处理含Cd(II)废水后, 混合菌中的优势菌属包括 *Comamonas* (39.94%)、*unclassified_f_Enterobacteriaceae* (34.96%)、*Ochrobactrum* (14.07%)、*Alcaligenes* (4.84%)、*Bordetella* (2.07%)、*Serratia* (1.04%)和 *Bacillus* (1.01%)。功能预测表明, 与代谢相关的基因丰度发生显著变化。该研究表明, 混合菌群具有处理含镉废水的潜力。

关键词: Cd(II); 废水处理; 细菌群落; 功能预测

(Edited by Wei-ping CHEN)